Effect of the concentration and carbon chain length of a sulfate-based surfactant on hydrate formation kinetics

Marvin Ricaurte, Jean-Philippe Torre, Joseph Diaz, Christophe Dicharry

To cite this version:

Marvin Ricaurte, Jean-Philippe Torre, Joseph Diaz, Christophe Dicharry. Effect of the concentration and carbon chain length of a sulfate-based surfactant on hydrate formation kinetics. 8th International Conference on Gas Hydrates (ICGH8), Jul 2014, Pékin, China. hal-02005618

HAL Id: hal-02005618
https://hal.science/hal-02005618

Submitted on 4 Feb 2019

HAL is a multi-disciplinary open access archive for the deposit and dissemination of scientific research documents, whether they are published or not. The documents may come from teaching and research institutions in France or abroad, or from public or private research centers.

L'archive ouverte pluridisciplinaire **HAL**, est destinée au dépôt et à la diffusion de documents scientifiques de niveau recherche, publiés ou non, émanant des établissements d'enseignement et de recherche français ou étrangers, des laboratoires publics ou privés.

Open Archive Toulouse Archive Ouverte

OATAO is an open access repository that collects the work of Toulouse researchers and makes it freely available over the web where possible

This is an author's version published in: http://oatao.univ-toulouse.fr/21878

Official URL:

To cite this version:

Ricaurte, Marvin and Torré, Jean-Philippe and Diaz, Joseph and Dicharry, Christophe *Effect of the concentration and carbon chain length of a sulfate-based surfactant on hydrate formation kinetics.* (2014) In: 8th International Conference on Gas Hydrates (ICGH8), 28 July 2014 - 1 August 2014 (Beijing, China).

Any correspondence concerning this service should be sent
to the repository administrator: tech-oatao@listes-diff.inp-toulouse.fr

*Proceedings of the 8th International Conference on Gas Hydrates (ICGH8-2014),
Beijing, China, 28 July - 1 August, 2014*

EFFECT OF THE CONCENTRATION AND CARBON CHAIN LENGTH OF A SULFATE-BASED SURFACTANT ON HYDRATE FORMATION KINETICS

Marvin RICAURTE, Jean-Philippe TORRÉ, Joseph DIAZ, Christophe DICHARRY [*]
Univ. Pau & Pays Adour, CNRS, TOTAL – UMR 5150 – LFC-R – Laboratoire des Fluides Complexes et leurs Réservoirs, Avenue de l'Université, BP 1155 – PAU, F-64013, FRANCE

ABSTRACT

This paper reports an experimental study on the effect of the concentration and the carbon chain length of surfactants on the formation kinetics of gas hydrates in a *quiescent* CO_2/CH_4/water system. Sodium alkyl sulfates with different carbon chain length (C_8, C_{10}, C_{12}, C_{14}, C_{16} and C_{18}) were tested at different concentrations. The experiments were conducted in a batch configuration, at a temperature of 275 K and with an initial gas pressure of about 3.3 MPa. For each system studied, hydrate crystallization was triggered by suddenly injecting a small amount of THF (4,000 ppm) directly into the surfactant solution in contact with the gas-hydrate-former phase at 275 K and 3.3 MPa. The long induction time for hydrate formation usually observed for these systems at the pressure and temperature conditions used in this study was thus eliminated. The experimental results show that, of the six surfactants tested, *only* the sodium dodecyl (C_{12}) sulfate efficiently promotes the formation of CO_2-CH_4 binary hydrate under quiescent conditions. A minimum concentration of 500 ppm of the C_{12} surfactant was however necessary to obtain a beneficial effect on hydrate formation, and the rate of hydrate crystallization was observed to level off for the surfactant concentrations higher than 3,000 ppm. For the systems containing the C_8 and C_{10} surfactants, which have a Krafft temperature lower than 275 K, the presence or absence of micelles in the surfactant solution does not have any effect on the hydrate formation kinetics.

Keywords: gas hydrates, crystallization, kinetics, surfactants, THF

NOMENCLATURE

c_s	Surfactant solubility [ppm]
i	Superscript referring to CO_2 or CH_4
$n_{g,r}$	Mole number of gas enclathrated in the hydrate phase [mol]
$(n_{g,r})_{Tot}$	Total mole number of gas enclathrated in the hydrate phase [mol]
t	Time [s]
t_{final}	Final time of the experiment [s]
t_{init}	Initial time of the experiment [s]
y^i	Molar concentration of the component i in the gas mixture [mol.m^{-3}]
z	Compressibility factor [-]
CMC	Critical micelle concentration [ppm]
N_c	Number of carbons in the surfactant alkyl chain [-]
P	Pressure [MPa]
R	Gas constant [J.K^{-1}.mol^{-1}]
T	Temperature [K]
T_k	Krafft temperature [K]
T_{targ}	Target temperature for hydrate formation [K]
V	Volume [m^3]
$\Delta n_{g,r}/\Delta t$	Gas enclathration rate [mol.min^{-1}]
$(\Delta n_{g,r}/\Delta t)_{Max}$	Maximum gas enclathration rate [mol.min^{-1}]
[C]	Concentration [ppm]

---

[*] Corresponding author: Phone: +33 5 5940 7682 Fax +33 5 5940 7695 E-mail: christophe.dicharry@univ-pau.fr

INTRODUCTION

The use of gas hydrate-based processes has been envisaged for various applications such as refrigeration [1], seawater desalination [2], and gas separation [3]. Achieving high enough rate of hydrate formation is generally one of the key challenges for an economically viable application of such processes. Acceleration of the hydrate formation rate can be obtained by using surfactants, such as SDS (sodium dodecyl sulfate, referred to as $SC_{12}S$ in the rest of the study) [4,5], or mixtures of surfactants (e.g. SDS) and thermodynamic hydrate promoters, such as tetrahydrofuran (THF) [3,6-8]. The promotion effect of these additives, or mixture of additives, may be remarkable especially in the absence of mechanical agitation (i.e. under quiescent conditions) [6-9]. In the presence of $SC_{12}S$, we observed that a porous hydrate structure, instead of a rigid hydrate film, forms at the (quiescent) water/gas (w/g) interface, spreads up the reactor walls and sucks up the remaining water by capillarity [5,8]. Therfore, the high exchange area maintained between the gas and water phases fosters ongoing hydrate crystallization. This mechanism of hydrate formation is referred to as "capillary-driven" [7,9,10].

In the present study, the influence of carbon chain length and concentration of sodium alkyl sulfates on the hydrate growth rate were experimentally investigated. All the experiments were conducted under *quiescent conditions*. To trigger the hydrate crystallization, we used an experimental method developped in a recent work [11], which consists in injecting a small amount of a liquid gas hydrate former (here THF) into the aqueous phase of the studied system, equilibrated at given pressure and temperature conditions inside the hydrate stabilty zone.

EXPERIMENTAL SECTION

Materials

Gas hydrates were formed with a gas mixture, composed of 75.02 ± 0.50 mol% of CO_2 and 24.98 ± 0.50 mol% of CH_4, supplied by Air Liquide. THF (purity > 99.9%) and $SC_{12}S$ (purity > 98%) were supplied by Sigma-Aldrich and Chem Lab, respectively. The others sodium (C_8, C_{10}, C_{14}, C_{16} and C_{18}) alkyl sulfates (purity of 99%, excepted for C_{14} (purity of 95%)) were supplied by Alfa Aeser. The values of the critical micelle concentration (CMC) in pure water at 298 K and the Krafft temperature (T_k) of these surfactants are given in Table 1. Pure water (resistivity of 18.2 MΩ.cm) produced by a laboratory water-purification system from Purelab was used to prepare the surfactant solutions.

Surfactant	**SC_8S**	**$SC_{10}S$**	**$SC_{12}S$**	**$SC_{14}S$**	**$SC_{16}S$**	**$SC_{18}S$**
CMC /ppm	30,660 [12,13]	8,721 [12,13]	2,300 [14]	699 [12,13]	189 [15]	60 [15]
Krafft point /K	<274	<274	289	311	317	325
[C] /ppm	2420	2710	3,000	3,190	3,590	3,880
	1.3 x CMC					

Table 1 Critical micelle concentrations (from literature data) and Krafft temperatures (measured in this work) of the sodium alkyl sulfates, and surfactant concentrations used for the hydrate formation experiments.

Apparatus

The experimental setup used for hydrate formation is depicted schematically in Figure 1. The hydrate-forming cell is a jacketed cylindrical vessel in titanium with an internal volume of 299.7 ± 0.9 cm^3. It has two sapphire windows of diameter 20 mm, and a star-shaped magnetic agitator for stirring. A jacketed gas-storage vessel and a high-pressure syringe pump (ISCO 100 DM) are used respectively to load the gas mixture and inject the THF into the cell.

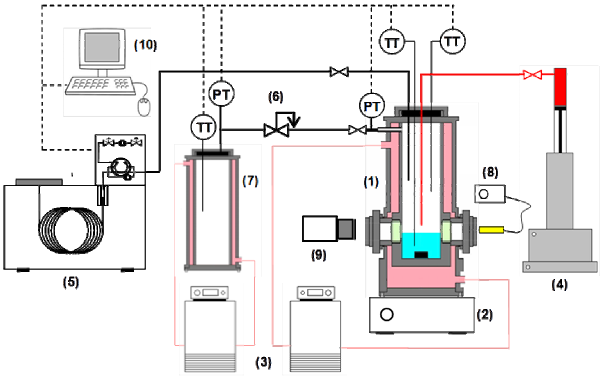

Figure 1 Schematic diagram of the experimental setup. (1) hydrate forming cell; (2) magnetic agitator; (3) thermostatic baths; (4) syringe pump; (5) gas chromatograph; (6) pressure reducing valve; (7) gas storage vessel; (8) lighting system; (9) video camera; (10) data acquisition system.

A gas chromatograph (Agilent, Model GC6980), connected to the cell, can be used to sample and analyze the gas phase composition. The gas and liquid temperatures in the cell are measured using PT100 probes with an accuracy of ± 0.2 K, and the cell pressure is measured with a 0–10 MPa pressure transducer accurate to within ± 0.02 MPa. The pressure and temperatures are recorded every second by a computer running an in-house LabView® program. During the experiments, the hydrate crystallization is visualized and recorded via a CCD camera connected to a computer.

Experimental procedure

Hydrate formation/dissociation experiments.

The cell is loaded with 65.0 ± 0.1 cm^3 of an aqueous solution containing the surfactant to be tested, then purged twice with the CO_2/CH_4 gas mixture to remove the remaining air present in the system, and then pressurized with 4.0 MPa of the gas mixture, at 293 K (these pressure and temperature conditions are outside the hydrate stability zone). The level of the surfactant solution in the cell reaches the middle of the sapphire windows and the tip of the tubing used for THF injection is located in the gas phase a few millimetres above the w/g interface. The agitator is started and set to 600 RPM, and the cell is cooled at a rate of 0.9 K/min to the target temperature $T_{targ} = 275$ K. One hour after the pressure has reached a constant value (about 3.3 MPa) at that temperature, the agitator is stopped (the hydrate formation experiment is thus conducted under *quiescent conditions*) and 0.30 ± 0.01 cm^3 of THF is injected in one shot at the rate of 10 cm^3/min with the syringe pump. This quantity represents a THF concentration of 4,000 ppm (by weight) in the aqueous phase. In the cell, temperature is maintained at T_{targ} until pressure stabilizes. Finally, the cell temperature is raised to 293 K at a rate of 1.5 K/min.

Krafft point determination. The Krafft point (i.e. the temperature below the surfactants cannot form micelles) was determined for each surfactant (Table 1) using a heating step method. Test tubes containing 10.0 ± 0.1 cm^3 of the surfactant solutions at the concentration of 10×CMC (at ambient temperature) are placed in a temperature-controlled bath at 274 K ($<T_{targ}$). At these conditions of temperature and concentration, only the SC_8S and $SC_{10}S$ surfactants are not in crystalline form. Bath temperature is maintained at this temperature for 24 h and then increased by step of 1 K every 24 h until all the surfactant solutions appear limpid. Before each increase of bath temperature, the test tubes are shaken moderately The Krafft point of a given surfactant is then defined as the temperature at which the solid particles of the surfactant are no longer visible with the naked eye. The uncertainty of the measured T_k value is ±1K. Note that the Krafft point under gas hydrate forming conditions is known not to shift from the Krafft point under atmospheric pressure [14,16].

RESULTS AND DISCUSSION

Effect of $SC_{12}S$ on the hydrate formation rate

The variation in cell pressure and cell temperature during an experiment with 3,000 ppm $SC_{12}S$ is shown in Figure 2a. From point A to B, the cell is cooled from 293 to 275 K (T_{targ}). The decrease in cell pressure resulting from this variation of temperature is caused by both gas contraction and solubilization of the gases (mainly CO_2). Once the pressure in the cell stabilizes, THF is injected into the $SC_{12}S$ solution. This injection causes, a few seconds later, a sharp rise of the cell temperature due to the onset of the hydrate crystallization. A few minutes later (point D) a second increase of the cell temperature is observed. The transient THF supersaturation produced at the injection point in all probability triggers the formation of a first hydrate, probably a mixed hydrate containing THF, CO_2 and CH_4, which then acts as seeds for the formation of the CO_2–CH_4 binary hydrate. The steep decrease in cell pressure observed after point D' reflects the formation of a large quantity of hydrate. At point E, temperature and pressure in the cell do not vary anymore, and the pressure value very well matches that of the CO_2–CH_4 binary hydrate calculated with the empirical correlation of Adisasmito et al. [17] using the gas composition measured at this point (see the full square in Figure 2a). The cell is then heated from 275 to 293 K to decompose the hydrates formed.

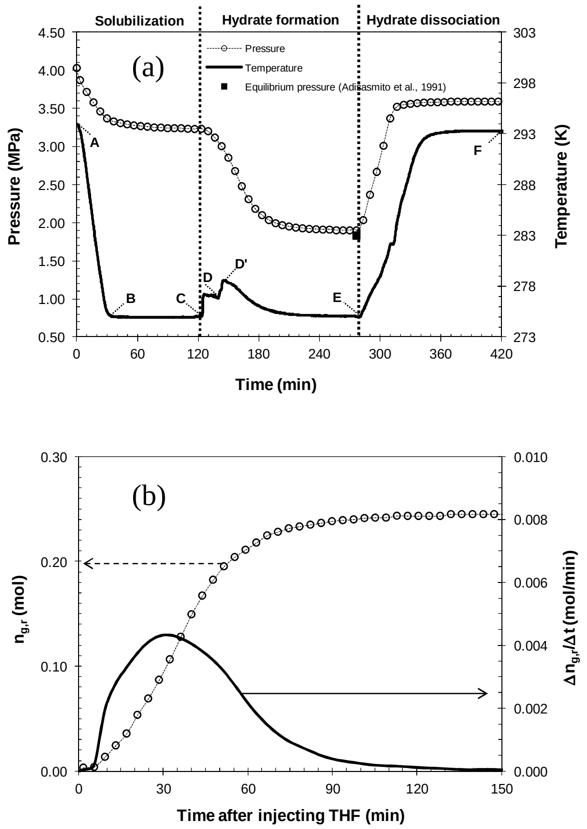

Figure 2 Typical curves obtained when injecting THF to trigger the hydrate crystallization: (a) cell pressure and cell temperature as a function of time; (b) mole number of gas enclathrated in the hydrate phase and gas enclathration rate as a function of time. Conditions are: $[SC_{12}S]$ = 3,000 ppm and $[THF]_{injected}$ = 4,000 ppm

Figure 2b shows the mole number of gas enclathrated in the hydrate phase, $n_{g,r}$ and the gas enclathration rate, $\Delta n_{g,r}/\Delta t$ as a function of time, with t = 0 min corresponding to the THF injection point and Δt is taken as 3.40 min.

$n_{g,r}$ is calculated using equation (1):

$$n_{g,r} = \sum_i n^i_{g,r} \qquad (1)$$

with

$$n^i_{g,r} = n^i_g\Big|_{t_{init}} - n^i_g\Big|_{t_{final}} = \frac{y^i PV}{zRT}\Big|_{t_{init}} - \frac{y^i PV}{zRT}\Big|_{t_{final}} \qquad (2)$$

where the compressibility factor z is calculated using the Peng Robinson equation of state.

The gas begins to be consumed by the hydrate phase almost immediately after the THF injection. $\Delta n_{g,r}/\Delta t$ reaches a maximum value about 30 minutes after the THF injection, and then decreases to almost zero about 100 minutes after the peak.

Figure 3 shows the total mole number of gas enclathrated in the hydrate phase $(n_{g,r})_{Tot}$ and $(\Delta n_{g,r}/\Delta t)_{Max}$ as a function of $SC_{12}S$ concentration.

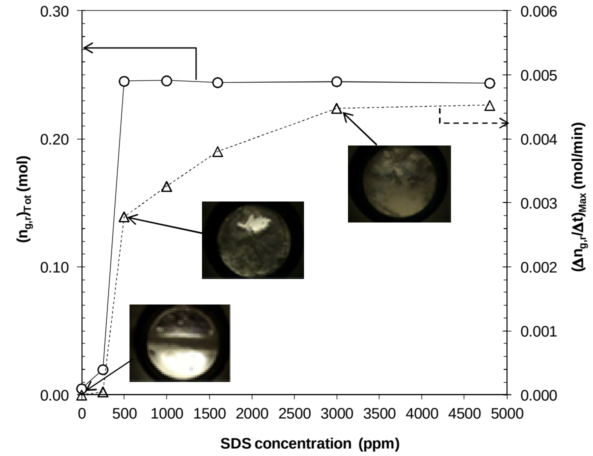

Figure 3 Total mole number of gas enclathrated in the hydrate phase and maximum gas enclathration rate as a function of $SC_{12}S$ concentration.

In the absence of $SC_{12}S$, hydrate forms a crust at the w/g interface (see the inserts in Figure 3 or the snapshots WS in Figure 4). The hydrate crust slightly grows downward (below the w/g interface) probably due to the presence of the CO_2 solubilized in the water phase. Ten minutes after the beginning of the hydrate crystallization, the crust is a few millimeters thick. Its thickness remains almost unchanged for the rest of the experiment. The crust breaks the contact between the water phase and the gas phase and, thus, hydrate growth stops. In this case $(n_{g,r})_{Tot}$ and $(\Delta n_{g,r}/\Delta t)_{Max}$ are almost zero.

In the presence of $SC_{12}S$, we observed a completely different behavior of the system. The hydrate phase growths on the w/g interface before expanding upward and downward (see the inserts in Figure 3 or the snapshots C12 in Figure 4). However, at least 500 ppm of SDS appears to be necessary for $(n_{g,r})_{Tot}$ and $(\Delta n_{g,r}/\Delta t)_{Max}$ to reach significant values: $(n_{g,r})_{Tot}$ takes a constant value of about 0.25 mol for all concentrations tested higher than 500 ppm, whereas $(\Delta n_{g,r}/\Delta t)_{Max}$ gradually increases before reaching a maximum value at 3,000 ppm of $SC_{12}S$. Okutani et al. [9] observed same tendencies for the effect of $SC_{12}S$ on CH_4-hydrate growth rate, namely: *(i)* a minimum concentration of $SC_{12}S$ (125 ppm in their case) is necessary to form significant amount of hydrate, *(ii)* the gas consumption rate increases with the surfactant concentration and then reaches a constant value (from 1000 ppm of $SC_{12}S$ in their case), and *(iii)* the total amount of gas consumed is almost the same irrespective of the $SC_{12}S$ concentration (provided the concentration is higher than the above-mentioned minimum concentration).

Effect of carbon chain length

In these experiments, the surfactants were used at two different concentrations: 188 ppm (mol), which corresponds to 3,000 ppm (wt) of $SC_{12}S$, and 1.3 times the CMC (see Table 1). Each experiment at the surfactant concentration of 188 ppm (mol) was duplicated.

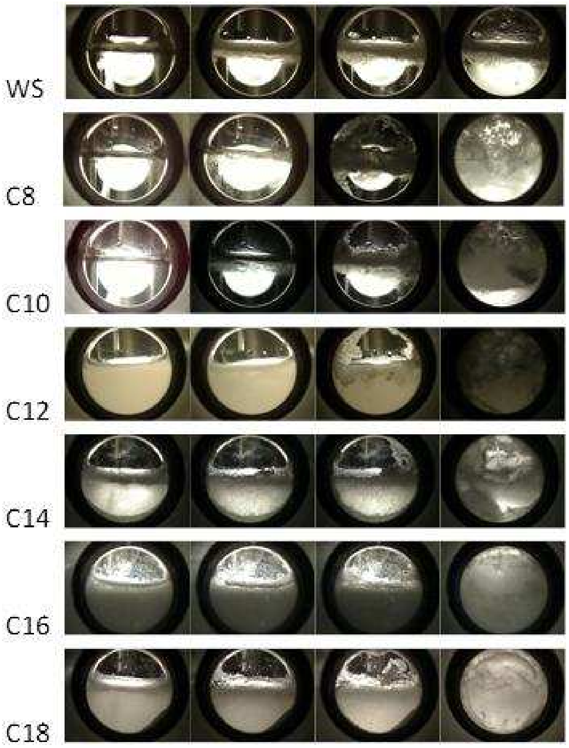

Figure 4 Snapshots of the systems containing 188 ppm (mol) of the sodium alkyl sulfate surfactants at 275 K. WS corresponds to the system without surfactant. The snapshots were taken at t = 0, ~1/4, 1 and 10 minutes after injecting THF.

It is worth noting that both concentrations used are higher than the CMC of the surfactants containing 12 to 18 carbons in their alkyl chain. These surfactants are, therefore, in a crystalline form at T_{targ}, since their Krafft points are higher than 275 K (Table 1). This can be clearly observed in the snapshots shown in Figure 4. At t = 0, one can see that the $SC_{12}S$ to $SC_{18}S$ surfactant solutions are turbid.

The solubility (c_s) beyond which the surfactant molecules form a hydrated solid in an aqueous solution at 275 K is reported to be 2,200 ppm (wt), 300 ppm and 40 ppm for $SC_{12}S$, $SC_{14}S$ and $SC_{16}S$, respectively [18]. Using the following empirical equation (3), which has been deduced from experimental solubility points from Watanabe et al. [18], the solubility of $SC_{18}S$ is estimated to be 6 ppm.

$$c_s = 4.10^8 \exp(-1.002 N_c) \qquad (3)$$

Therefore, the amount of solubilized surfactant molecules available to readily adsorb at the hydrate surface at T_{targ} is much smaller for the $SC_{12}S$-$SC_{18}S$ surfactants than for the SC_8S and $SC_{10}S$ ones.

Same hydrate formation mechanism observed for the system with $SC_{12}S$ occurs in the presence of the other sodium alkyl sulfates too (see the snapshots Figure 4). However, ten minutes after triggering the hydrate crystallization, the hydrate phase that covers the sapphire windows appears much more dark for the $SC_{12}S$ system suggesting a higher amount of hydrate formed in this case. This is confirmed in Figure 5, where $(n_{g,r})_{Tot}$ is plotted as a function of the carbon chain length. In the presence of $SC_{12}S$, the total mol number of gas enclathrated in the hydrate phase is 20 to 25 higher than with the other surfactants and about 35 times that with pure water. Excepted for the $SC_{12}S$ systems, the hydrate growth rate is very slow and, therefore, the values of $(\Delta n_{g,r}/\Delta t)_{Max}$ are almost zero. The same hydrate formation behavior is observed at both surfactant concentrations used.

Despite fewer solubilized molecules, $SC_{12}S$ shows better performance at promoting and accelerating hydrate formation than the SC_8S and $SC_{10}S$ surfactants. The presence of micelles at the highest concentration tested for SC_8S and $SC_{10}S$ does not change the result. It suggests that the ability of $SC_{12}S$ to adsorb at the hydrate surface and/or to prevent the hydrate particles from agglomerating is much higher than that of the surfactants of the same family with a shorter alkyl chain. One may have expected that the longer alkyl chain of the $SC_{14}S$, $SC_{16}S$ and $SC_{18}S$ surfactants would have provided better protection against particle agglomeration and thus good hydrate promotion and acceleration. However, the amount of solubilized molecules, and thus of molecules adsorbed at the hydrate surface, is probably too small for these surfactants to produce good performance.

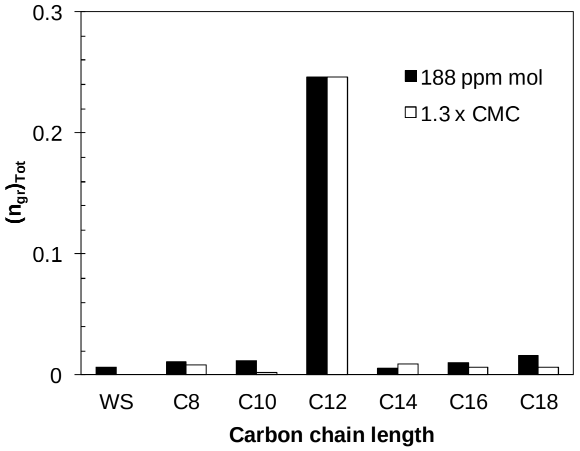

Figure 5 Total mole number of gas enclathrated in the hydrate phase as a function of the surfactant carbon chain length.

The results obtained in this work for $SC_{14}S$ and $SC_{16}S$ contrast with those reported by Okutani et al. [9], who found that these surfactants produced almost equivalent promotion as $SC_{12}S$. As in our experiments, they used quiescent conditions and the same temperature (275 K) for hydrate formation. The main differences in their work were, the use of CH_4 as gas hydrate former and lower surfactant concentrations (from 50 to 600 ppm for $SC_{14}S$ and 10 to 150 ppm for $SC_{16}S$).

We know from different works (not published) conducted in our laboratory on the promotion effect of $SC_{12}S$ that it is less effective at promoting the formation and growth of CO_2-hydrate than CH_4-hydrate. These different behaviors could result from the fact that the $C_{12}S^-$ adsorption behavior depends on the nature of the hydrate formers [19]. When the hydrate former is hydrophobic, the tail of $C_{12}S^-$ would lay down on the hydrate surface [19,20], whereas for hydrophilic hydrate former it would stand up on the hydrate surface [21]. Because effective protection of hydrate particles against agglomeration is expected to depend on the surfactant coverage of the hydrate surface, more adsorbed molecules should be necessary to prevent "hydrophilic" hydrate particles from agglomerating. The high proportion of CO_2 of the gas mixture used in our work and the injection of THF (which is a polar hydrate former) to trigger the hydrate crystallization might be responsible for the difference observed for $SC_{14}S$ and $SC_{16}S$ as compared to the results obtained by Okutani et al. [9]. Another possible reason for the differences observed could be the relatively high surfactant concentrations used here. Several studies reported that the promotional effect of surfactants shows a maximum at a certain concentration but decrease with further concentration increases [3,9,22]. We will use lower concentration of $SC_{14}S$ and $SC_{16}S$ to verify this hypothesis in a future work.

CONCLUSION

The effects of carbon chain length and concentration of sodium alkyl sulfate surfactants (SC_nS, with n = 8, 10, 12, 14, 16 and 18) on the hydrate formation rate in a *quiescent* CO_2/CH_4/water system were experimentally examined. All the surfactants used produce visually the same change in hydrate-formation behavior. Unlike the system without surfactant, where a hydrate crust forms at the w/g interface, the hydrate phase growths on the w/g interface before expanding upward and downward when surfactant is present. However, only $SC_{12}S$ was found to drastically increases the hydrate formation rate. It also increases the amount of hydrate formed. The acceleration effect reaches a maximum at the concentration of ~ 3,000 ppm, whereas the amount of hydrate formed reaches a maximum at ~ 500 ppm of $SC_{12}S$ in the system.

The incapability of the other surfactants tested to effectively promote the hydrate formation might be due to: *(i)* a poorer anti-agglomerant property of the surfactants with 8 and 10 carbons in the alkyl chain, that prevent the “capillary-driven” hydrate formation mechanism from developing, *(ii)* a too low coverage of the hydrate surface by the surfactants with 14, 16 and 18 carbons, due to both their low in-water solubility at the temperature of 275 K used in this work to form hydrates and to the configuration of the surfactant molecules adsorbed at the hydrate surface .

REFERENCES

[1] Clain P., Delahaye A., Fournaison L., Mayoufi N., Dalmazzone D., Fürst W. *Rheological properties of tetra-n-butylphosphonium bromide hydrate slurry flow.* Chem. Eng. J. 2012;193-194:112-122.

[2] Wang L., Zhang X., Li H., Shao L., Zhang D., Jiao L. *Theory research on desalination of brackish water using gas hydrate method.* Advanced Materials Research 2013;616-618:1202-1207.

[3] Ricaurte M., Dicharry C., Broseta D., Renaud X., Torré J.-P. *CO_2 removal from a CO_2-CH_4 gas mixture by clathrate hydrate formation using THF and SDS as water soluble hydrate promoters.* Ind. Eng. Chem. Res. 2013; 52 (7):899-910.

[4] Zhong Y., Rogers R.E. *Surfactant effects on gas hydrate formation.* Chem. Eng. Sci. 2000;55(19): 4175-4187.

[5] Gayet P., Dicharry C., Marion G., Graciaa A., Lachaise J., Nesterov A. *Experimental determination of methane hydrate equilibrium curve up to 55 MPa by using a small amount of surfactant as hydrate promoter*. Chem. Eng. Sci. 2005;60(21):5751-5758.

[6] Tang J., Zeng D., Wang C., Chen Y., He L., Cai N. *Study on the influence of SDS and THF on hydrate-based gas separation performance*. Chem. Eng. Res. Des. 2013;91(9):1777-1782.

[7] Torré J.-P., Ricaurte M., Dicharry C., Broseta D. *CO_2 enclathration in the presence of water-soluble hydrate promoters: hydrate phase equilibria and kinetics studies in quiescent conditions*. Chem. Eng. Sci. 2012;82:1-13.

[8] Ricaurte M., Dicharry C., Renaud X., Torré J.-P. *Combination of surfactants and organic compounds for boosting CO_2 separation from natural gas by clathrate hydrate formation*. Fuel 2014;122:206-217.

[9] Okutani K., Kuwabara Y., Mori Y.H. *Surfactant effects on hydrate formation in an unstirred gas/liquid system: an experimental study using methane and sodium alkyl sulfates*. Chem. Eng. Sci. 2008;63(1):183-194.

[10] Yoslim J., Linga P., Englezos P. *Enhanced growth of methane-propane clathrate hydrate crystals with sodium dodecyl sulfate, sodium tetradecyl sulfate, and sodium hexadecyl sulfate surfactants.* J. Crystal Growth 2010;313:68-80.

[11] Ricaurte M., Torré J.-P., Diaz J., Dicharry C. *In situ injection of THF to trigger gas hydrate crystallization: application to the evaluation of a kinetic hydrate promoter*. Chem. Eng. Res. Des. 2014;http://dx.doi.org/10.1016/j.cherd.2013.12.007.

[12] Varga I., Meszaros, R., Gilanyi T. *Adsorption of sodium alkyl sulfate homologues at the air/solution interface*. J. Phys. Chem. B 2007;111:7160-7168.

[13] Ranganathan R., Tran L., Bales B. *Surfactant and salt-induced growth of normal sodium alkyl sulfate micelles well above their critical micelle concentrations*. J. Phys. Chem. B 2000;104:2260-2264.

[14] Zhang J.S., Lee S., Lee J.W. *Does SDS micellize under methane hydrate-forming conditions below the normal Krafft point?* J. Colloid Interface. Sci. 2007;315:313-318.

[15] SIDS Initial Assessment Report for SIAM 25. October 16-19 2007, Helsinki. http://www.aciscience.org/docs/alkyl_sulfates_siar.pdf

[16] Zhang J.S., Lee S., Lee J.W. *Solubility of sodium dodecyl sulfate near propane and carbon dioxide hydrate-forming conditions.* J. Chem. Eng. Data 2007;52(6):2480-2483.

[17] Adisasmito S., Frank R.J., Sloan E.D. *Hydrates of carbon dioxide and methane mixtures*. J. Chem. Eng. Data. 1991;36;68-71.

[18] Watanabe K., Niwa S., Mori Y.H. *Surface tensions of aqueous solutions of sodium alkyl sulfates in contact with methane under hydrate-forming conditions*. J. Chem. Eng. Data 2005;50:1672-1676.

[19] Lo C., Zhang J.S., Somasundaran P., Lu S., Couzis A., Lee J.W. *Adsorption of surfactants on two different hydrates*. Langmuir 2008;24(22):12723-12726.

[20] Lo C., Zhang J.S., Couzis A., Somasundaran P., Lee J.W. *Adsorption of cationic and anionic surfactants on cyclopentane hydrates*. J. Phys. Chem. C 2010;114(31):13385-13389.

[21] Zhang J.S., Lo S., Somasundaran P., Lu S., Couzis A., Lee J.W. *Adsorption of sodium dodecyl sulfate at THF hydrate/liquid interface*. J. Phys. Chem. C 2008;112(32):12381-12385.

[22] Daimaru T., Yamasaki A., Yanagisawa Y. *Effect of surfactant carbon chain length on hydrate formation kinetics*. J. Petrol. Sci. Eng. 2007;56:89-96.